Chemical Engineering Journal 147 (2009) 307–315

Contents lists available at ScienceDirect

Chemical Engineering Journal

journal homepage: www.elsevier.com/locate/cej

Positive and negative catalytic effects of a nickel mesh catalyst for the partial oxidation of ethane

Syed Shatir Asghrar Syed-Hassan, Woo Jin Lee, Chun-Zhu Li*

Department of Chemical Engineering, PO Box 36, Monash University, Victoria 3800, Australia

ARTICLE INFO

Article history:
Received 5 August 2008
Received in revised form
13 November 2008
Accepted 14 November 2008

Keywords:
Radical desorption
Mass transfer of radicals
Catalytic partial oxidation
Ethane
Nickel mesh catalyst

ABSTRACT

The catalytic reactions between O_2 and hydrocarbons are an important class of reactions in energy and chemical industries. This study aims to investigate the complicated reactions involving reactive radicals on the catalyst surface and in the gas phase during the partial oxidation/combustion of light alkanes. In order to avoid intra-particle transport constraints associated with the traditional porous catalysts, a non-porous nickel mesh catalyst has been used in this study for the partial oxidation of ethane with O_2 at 625 °C at atmospheric pressure. The catalytic effects of the nickel mesh strongly depended on the flow rate of gas reactants passing through the mesh. At a low gas flow rate, the nickel mesh catalyst showed negative effects for the oxidation of ethane. At a high gas flow rate, the same catalyst showed positive catalytic effects. Our results can be explained by considering the selective/preferential adsorption and desorption of different radicals onto and from the catalyst surface. It is believed that the desorption of some surface generated radicals (e.g. OH radicals) may be greatly affected by the thickness of the mass transfer gas film around the mesh wires, which in turn is affected by the gas flow rate passing through the mesh.

© 2008 Elsevier B.V. All rights reserved.

1. Introduction

The catalytic reactions between O_2 and hydrocarbons are an important class of reactions in energy and chemical industries. The catalytic combustion of natural gas promises to reduce the emissions of air pollutants drastically. The catalytic partial oxidation of alkanes with O_2 remains a potential clean alternative to the energy-intensive steam cracking of light alkanes [1] in the production of alkenes, especially ethylene and propylene whose demands continue to raise [2].

Traditionally, catalysts in the form of porous particles are normally employed for this type of gas–solid reactions. There are, however, some great disadvantages associated with the use of porous catalysts especially for fast reactions such as hydrocarbon–O_2 reactions at high temperature. The reaction system can easily become rate-limited by mass and/or heat transfer.

At high temperature, the catalytic reactions of hydrocarbon–O_2 mixture are exceedingly complex. The reactions involving numerous radicals take place both in the gas phase and on the catalyst surface. Significant evidence [3–12] exists to show that surface-generated radicals do not always continue their reactions on the catalyst surface but can also desorb from the surface to participate in the gas-phase reactions both outside the catalyst particle as well as inside the catalyst pore itself.

When porous catalysts are used, the mass transfer limitation for reactive radicals inside the catalyst pores can become "irreducible" [13,14]. Unlike the molecular species, the elimination of transport limitations for highly reactive radical species would require particle sizes that are too small to be achieved practically, for example, based on pressure drop consideration. It then becomes a forbidden task to understand the inter-influence between the reactions on the catalyst surface and those "in the gas phase" within the pores of a catalyst particle.

The dual roles of catalyst surface in generating and quenching the radical intermediates [9,12–15] brings further intricacy in evaluating the exact contributions of homogeneous and heterogeneous pathways to the overall reaction mechanism. When the radicals generated on the catalyst surface desorb into the gas phase, these radicals may initiate and speed up the gas-phase radical reactions. The catalyst would thus show positive effects on the observed reaction rates [3–5,10]. On the other hand, when the radicals generated in the gas phase adsorb onto the catalyst surface [16], the chain of radical reactions in the gas phase would be effectively shortened. The catalyst would then show negative effects on the observed reaction rates.

For a non-porous mesh catalyst, the absence of a complicated internal porous structure means the automatic elimination of intra-particle diffusion resistance for the radicals, which would otherwise exist for a porous catalyst. Our previous studies [8–12] using non-

* Corresponding author. Tel.: +61 3 9905 9623; fax: +61 3 9905 5686.
E-mail address: chun-zhu.li@eng.monash.edu.au (C.-Z. Li).

1385-8947/$ – see front matter © 2008 Elsevier B.V. All rights reserved.
doi:10.1016/j.cej.2008.11.038

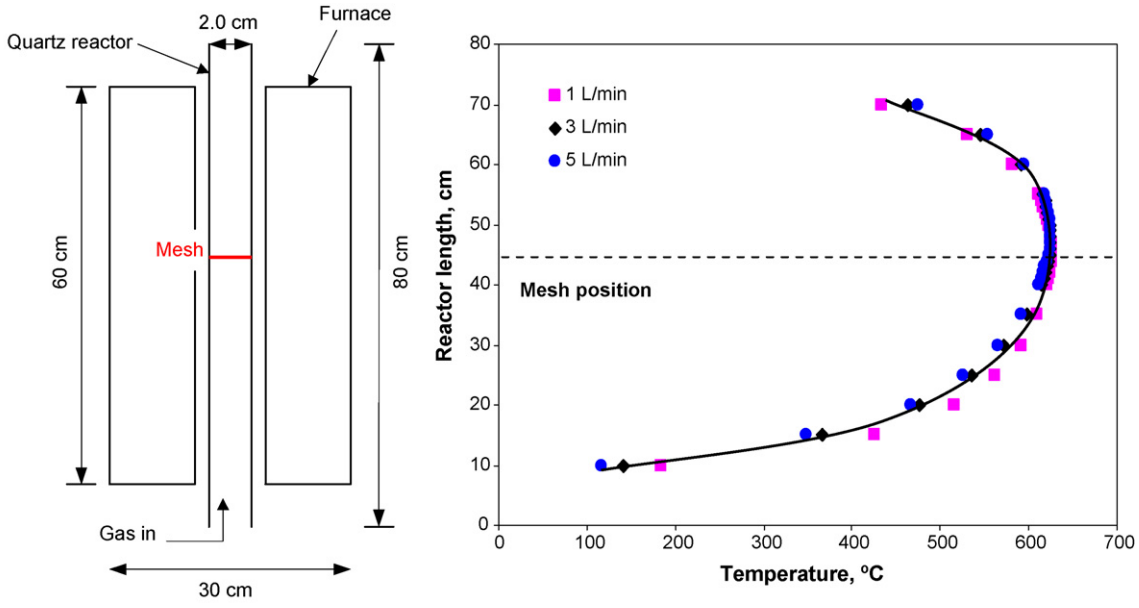

Fig. 1. Design of the reactor and its axial temperature distribution (measured from inside the quartz tube reactor).

porous mesh catalysts have shown that the desorption of radicals from the catalyst surface into the gas phase can be effectively facilitated by decreasing the gas film thickness around the mesh wires. This was achieved conveniently by increasing the gas flow rate passing through the mesh catalyst [8–12]. Clearly, the non-porous mesh catalysts provide a convenient means to examine the effects of radical adsorption/desorption on the mechanisms of hydrocarbon reactions which are often overlooked in kinetic studies.

We have demonstrated [8,12] that the desorption of radicals can not only change the observed reaction rates but also change the formation of carbon deposit on the catalyst surface. More recently, we have shown [17] that the desorption of radicals from the catalyst surface can be used to control/enhance the growth of carbon nanofibres. The focus of our previous studies [8–11,17] has mainly been on the adsorption and desorption of hydrocarbon radicals. In this study, we aimed to investigate the adsorption and desorption of radicals in the more complicated ethane–O_2 reaction system where hydrocarbon radicals together with O-containing radicals (e.g. OH radicals) are present. Both positive and negative catalytic effects of a nickel mesh catalyst have been observed for this reaction system. Our observations are explained by considering the preferential adsorption and desorption of C_2H_5 and OH radicals.

2. Experimental

The experiments were carried out in a quartz tube reactor identical to those previously described for the pyrolysis of ethane [12]. The reactor with an internal diameter of 2.0 cm and a length of 80 cm was placed and heated inside a 60 cm long single-heated-zone electrical furnace. The reactor was positioned so that 10 cm of its top and bottom were outside of the furnace (see Fig. 1). Reactant gases used were chemically pure grade ethane (99.00% purity) from BOC and the mixture of O_2 in argon balance (Coregas). The flow rates of the gases were controlled with mass flow controllers (Aalborg) separately and are reported throughout this paper as the flow rates under normal ambient condition (25 °C and 1 atm). With the pre-set ratios controlled by the mass flow controllers, all the gases were allowed to mix before being fed directly into the reactor from the bottom.

The reactor was operated both as a non-catalytic and a catalytic reactor. When it was used as a catalytic reactor, a nickel mesh (36% open area and 0.38 mm width opening) was used as a catalyst. The mesh (from Unique Co.) was weaved (40 × 40) using pure nickel wires of 0.25 mm diameter. A fresh round piece of nickel mesh with a diameter just slightly larger than 2.0 cm was used as the catalyst for each experiment. It was then washed with a mixture of methanol and chloroform to remove greases and impurities before being used. The mesh catalyst was placed inside the quartz tube, slightly above the middle of the reactor, which is the onset of isothermal zone as is shown in Fig. 1.

In this study, we also performed experiments using three layers of nickel mesh, 5 mm apart, as catalyst. In the presence of the first piece of mesh, the temperature at locations 5 and 10 mm above the first mesh was measured, confirming that all meshes would be in the isothermal zone, as expected from Fig. 1.

In each experiment, the reactor was heated slowly from room temperature to 625 °C in the isothermal zone after purging the reactor with the reactant gas. This temperature was chosen for this study because the non-catalytic reactions proceed significantly (but not excessively) under current experimental conditions. A significant extent of non-catalytic reactions is necessary in order to investigate the inter-influence between the reactions on the catalyst surface and those in the gas phase. The thermal expansion of the mesh during heating, being larger than that of quartz, ensured that the mesh catalyst remained at its intended position at all times during the course of the experiment. A K-type thermocouple was installed in contact with the mesh catalyst inside the quartz tube reactor to monitor the reaction temperature. Fig. 1 shows the axial temperature profile of the reactor and indicates the position of mesh catalyst during experiments. All experiments were run for more than 120 min, during which the reaction rates reached their plateau values.

After holding for 120 min, the reactor was immediately cooled to allow the mesh to drop to the bottom of the reactor. As soon as the mesh dropped, the temperature was once again raised to the same set temperature for the study of reactions without a catalyst (blank experiment). During the blank experiment, the thermocouple remained inside the reactor at the same location as in the corresponding catalytic experiment.

Reaction products were analysed using two different gas chromatography (GC) systems. An HP 5890 GC equipped with a HayeSep DB column (15 ft × 1/8 in.) and a flame ionization detector (FID) was

used to quantify hydrocarbons in the product gases while other light gases were analysed using a PerkinElmer Autosystem XL GC with a molecular sieve column (1 m × 1/8 in.), a Porapak N (3 m × 1/8 in.) column and a thermal conductivity detector (TCD). The formation rates of various product species (other than H_2O) were calculated by considering the total gas flow rate and the concentration of the species as detected by the GCs. Each datum of product formation rate reported here represents an average of at least three samples taken after the reaction had reached its steady state during the same experiment.

3. Results and discussion

3.1. Gas-phase ethane oxidation

Extensive experiments with an empty reactor were carried out in order to understand the non-catalytic gas-phase reactions. Total gas flow rates were varied to see the effects of residence time on reactant conversion and product distributions. In all experiments, C_2H_6/O_2/Ar feed composition was 10/5/85 (by vol) and the temperature inside the reactor was kept constant at 625 °C. Fig. 2 shows product formation rates at different total gas flow rates.

Mechanisms describing gas-phase reactions of ethane oxidation have been proposed in previous studies [3,18–22]. A list of commonly accepted main elementary reactions in the absence of a catalyst is presented in Table 1. It should be emphasised that Table 1 is not meant to include hundreds of all possible elementary reactions but only to include the main reactions responsible for the formation and destruction of main products. In a purely homogenous system, two possibilities of ethane activation exist. Ethane can undergo unimolecular decomposition to form CH_3 radicals (1) or alternatively it may react with molecular oxygen to form C_2H_5 and HO_2 radicals (2). Using rate constant values in Table 1, the relative importance of radical initiations by reactions (1) and (2) can be estimated. Under our reaction conditions of 5.0% oxygen (6.8×10^{-4} mol/L), 625 °C and 1 atm

$$\frac{\text{rate}(1)}{\text{rate}(2)} = \frac{k_1}{k_2[O_2]} \approx 35$$

Therefore, reaction (1), followed by reaction (3), is the main initiation step of the radical chain reactions in the gas phase. It should be noted that the chain initiation through reactions (1) and (3) or through reaction (2) would lead to the same radical of C_2H_5 for further reactions.

The resulting ethyl radicals will then transform into ethylene by direct attack of oxygen molecule (4) or through its thermal decomposition (5). However, from the following expression:

$$\frac{\text{rate}(4)}{\text{rate}(5)} = \frac{k_4[O_2]}{k_5} \approx 4600$$

reaction (4) is the prevailing pathway for ethylene formation. The HO_2 radical produced by reaction (4) can abstract hydrogen from another ethane molecule to return an ethyl radical while producing hydrogen peroxide (6). Hydrogen peroxide acts as a chain branching agent whereby its decomposition through reaction (8) yields more reactive OH radicals [3,19]. As the reaction proceeds inside the reactor, the concentration of HO_2 radicals will increase rapidly and as a result, reaction (7) is promoted more than reaction (6) [18]. Likewise, the concentration of OH radicals will also increase and hence reaction (9) immediately becomes the primary reaction for ethane consumption [18].

From this mechanism in Table 1, it is obvious that OH radicals play crucial roles in the gas-phase reactions involving ethane and oxygen. Since this radical is very reactive, it will not only act as a hydrogen abstractor from ethane molecules (9) but also responsible for further degradation of C_2H_4 which ultimately leads to the formation of CO, CO_2 and H_2 as terminal products as is described in Table 1.

In our study, the oxidation of ethane in the empty reactor shows typical behaviour of a radical chain process. As is shown in Figs. 2 and 3, the gas-phase non-catalytic reaction rates, labelled as "blank", were observed to increase monotonically with decreases in the total gas flow rate. This implies that the gas-phase reactions were profoundly dependent on the concentrations of various free radicals [18]. During a blank experiment at a high gas flow rate, the short residence time did not generate radicals at concentrations high enough to allow the reactions to take place at high rates. Short residence time also means that the radicals and the reactants did not have enough time to react in the heated zone. At high gas flow rates (>2.0 L min^{-1}) where C_2H_6 conversion was found to be very low, C_2H_4 turned out to be practically the only C-containing product species. As the conversion increased with increasing residence time, other species started to show up in the product gas. Changes in product selectivities (Fig. 4) are mainly attributed to the degradation of C_2H_4 through reactions (18)–(26) as the gas spent relatively longer time inside the reactor. As presented in Table 1, the pathway for C_2H_4 degradation involves OH radical attack to yield CO_x, H_2 and H_2O via various intermediates such as C_2H_3, CH_3 and CH_2O.

3.2. Catalytic partial oxidation of ethane using a single layer of nickel mesh catalyst

Product formation rates in the presence of a single layer of mesh catalyst are also plotted in the same figure (Fig. 2) as for the blank experiments in order to facilitate comparison between catalytic and non-catalytic reactions. In contrast to the results obtained in the blank experiments where formation rates of all products increase monotonically with decreasing gas flow rate, reactions with the nickel mesh catalyst exhibit more complex patterns. From Fig. 2, the effects of nickel mesh catalyst can be broadly divided into two distinct regions. One is the lower flow rate region (<1.7 L min^{-1}) in which formation rates of hydrocarbon products particularly C_2H_4 were lower ("negative catalytic effects") than that obtained by the reactions without a catalyst. Another is the higher flow rate region (>1.7 L min^{-1}) where "positive catalytic effects" in term of product formation rates and reactant conversions were observed.

3.2.1. Quenching of radicals—negative catalytic effects of mesh catalyst

A careful comparison of reactant conversions between blank and catalytic experiments (Fig. 3) reveals that there was a slight decrease in the conversion of ethane in the catalytic experiments compared to the blank ones at the very low gas flow rates (<1.7 L min^{-1}). As can be seen from Fig. 2, significant amounts of product species were formed from the homogeneous non-catalytic reactions in this region. Mass balance calculation also indicated that appreciable amounts of H_2O (not shown in the graph) were also formed from the gas-phase reactions. The adsorption of product molecules (e.g. CO_2 and H_2O) onto the catalyst surface could have inhibited the reaction on the catalyst surface [11,23,24]. However, this inhibition could at most give similar C_2H_6 conversions, but would not cause decreases in C_2H_6 conversion as we observed experimentally (Fig. 3).

We believe that the presence of a nickel mesh has disrupted the chain reactions in the gas phase by providing a surface to catalyse the radical termination reactions, i.e. the "negative catalytic effect". More than one type of radical species could be quenched on the catalyst surface. However, the data in Fig. 2 show a bigger negative effect of catalyst on formation rates of C_2H_4 and other hydrocarbon products than other products. Therefore, hydrocarbon radicals would be quenched the most. Hydrocarbon radicals such as C_2H_5 and CH_3 formed in the gas phase upstream of the Ni mesh may

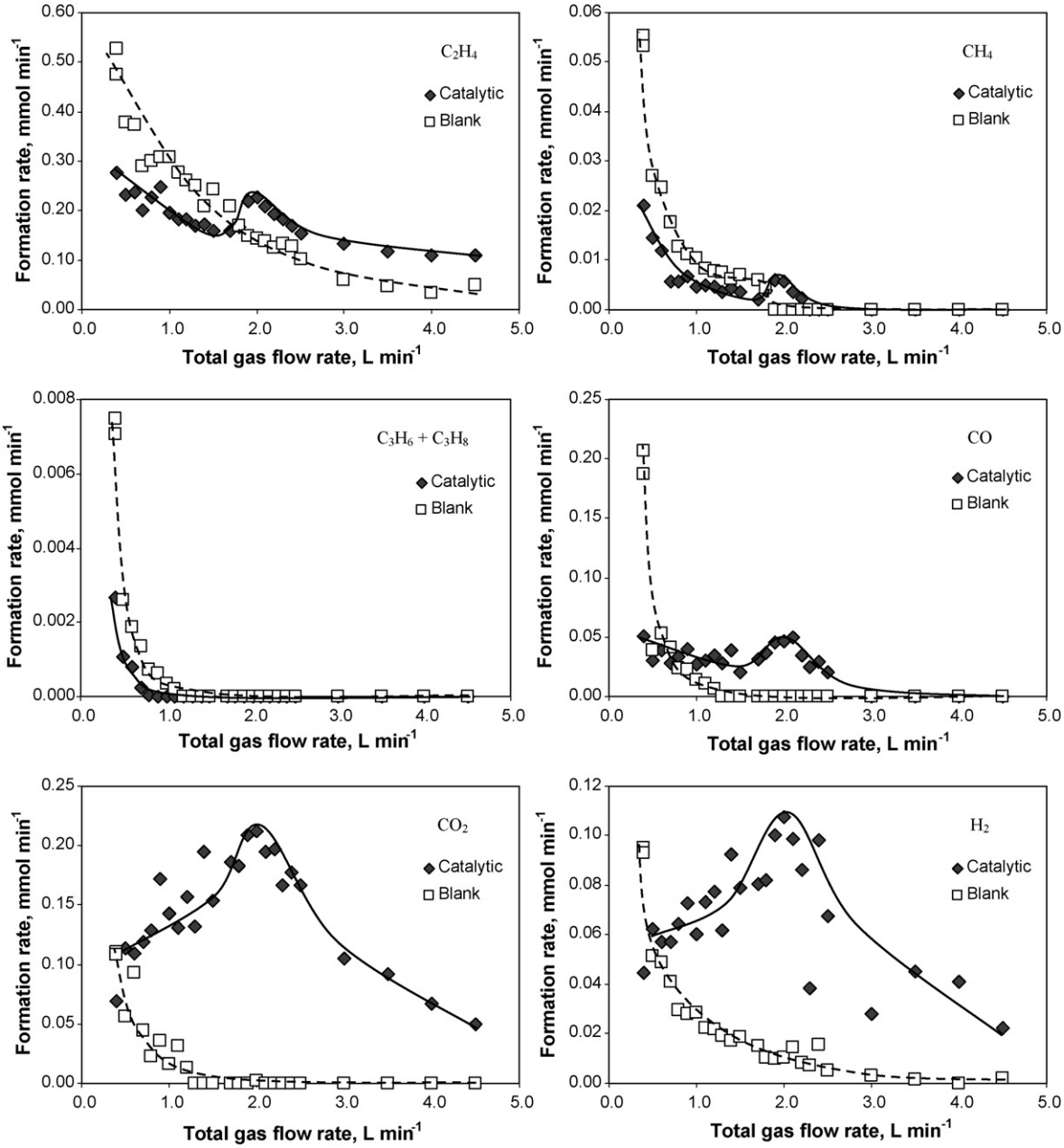

Fig. 2. Changes in product formation rates with the total gas flow rate from the catalytic and non-catalytic (blank) partial oxidation of ethane at 625 °C with the feed composition of $C_2H_6/O_2/Ar = 10/5/85$ (by vol) at atmospheric pressure.

collide with the catalyst surface to form alkoxide species. Collision between a methyl radical and catalyst surface is believed to result in the formation of surface methoxide [15]. Similarly, the collision of an ethyl radical with the nickel mesh catalyst covered by the adsorbed oxygen species in our study could result in the formation of surface ethoxy species:

$$CH_3(g) + O^-(s) = CH_3O(s) \quad (27)$$

$$C_2H_5(g) + O^-(s) = C_2H_5O(s) \quad (28)$$

The unstable surface ethoxide can be transformed to ethylene. However if ethylene fails to diffuse immediately into the bulk gas stream, reaction (29) can then be easily shifted to the right [25,26] to form thermodynamically more stable CO_x in the same way as that of the methoxide degradation (30) [15]:

$$C_2H_4(s) + OH(s) \leftrightarrow C_2H_5O(s) \rightarrow CH_3COO(s),\ HCOO(s) \rightarrow CO_x \quad (29)$$

$$CH_3O(s) \rightarrow HCOO \rightarrow CO_x \quad (30)$$

While the formation and degradation of surface alkoxide species, as outline above, may explain the increased formation of CO_2 (Fig. 2) in the presence of the mesh catalyst, other reactions on catalyst surface must be considered to account for the decreases in the ethane conversions due to the presence of the mesh catalyst as shown in Fig. 3. We suspect that C-containing radicals could adsorb on Ni surface and then recombine to form the original C_2H_6, e.g. through reactions (31) and (32):

$$CH_3(s) + CH_3(s) = C_2H_6(s) \quad (31)$$

Table 1
A list of main elementary gas-phase reactions and their rate constants under present experimental conditions.

Reaction		k (s^{-1} or $M^{-1}\,s^{-1}$ or $M^{-2}\,s^{-1}$) at 898 K	Refs
Initiation			
$C_2H_6 = CH_3 + CH_3$	(1)	9.17×10^{-5}	[21]
$C_2H_6 + O_2 = C_2H_5 + HO_2$	(2)	3.86×10^{-3}	[20]
$CH_3 + C_2H_6 = CH_4 + C_2H_5$	(3)	2.74×10^{6}	[21]
Propagation			
$C_2H_5 + O_2 = C_2H_4 + HO_2$	(4)	2.47×10^{7}	[20]
$C_2H_5 = C_2H_4 + H$	(5)	3.63×10^{0}	[39]
$HO_2 + C_2H_6 = C_2H_5 + H_2O_2$	(6)	6.30×10^{4}	[20]
$2HO_2 = H_2O_2 + O_2$	(7)	2.00×10^{9}	[21]
$H_2O_2 + M = 2OH + M$	(8)	1.01×10^{3}	[22]
$OH + C_2H_6 = H_2O + C_2H_5$	(9)	3.53×10^{9}	[21]
Termination			
$CH_3 + CH_3 = C_2H_6$	(10)	1.68×10^{10}	[20]
$C_2H_5 + C_2H_5 = C_2H_6 + C_2H_4$	(11)	1.40×10^{9}	[20]
$C_2H_5 + CH_3 = C_3H_8$	(12)	1.14×10^{10}	[40]
$C_2H_5 + CH_3 = C_2H_4 + CH_4$	(13)	2.43×10^{6}	[20]
$C_2H_5 + OH = C_2H_4 + H_2O$	(14)	2.41×10^{10}	[20]
$HO_2 + OH = H_2O + O_2$	(15)	2.00×10^{10}	[21]
Reactions leading to CO_x and H_2 formation			
$C_2H_5 + HO_2 = CH_3 + CH_2O + OH$	(16)	2.50×10^{10}	[20]
$C_2H_5 + OH = CH_3 + CH_2O + H$	(17)	2.41×10^{10}	[20]
$C_2H_4 + OH = CH_3 + CH_2O$	(18)	1.17×10^{9}	[22]
$C_2H_4 + OH = C_2H_3 + H_2O$	(19)	7.31×10^{8}	[21]
$C_2H_3 + OH = C_2H_2 + H_2O$	(20)	3.00×10^{10}	[21]
$CH_2O + OH = CHO + H_2O$	(21)	1.53×10^{10}	[21]
$C_2H_2 + OH = CH_3 + CO$	(22)	2.76×10^{10}	[22]
$CH_3 + OH = CH_2O + H_2$	(23)	1.03×10^{10}	[21]
$CH_3 + HCO = CH_4 + CO$	(24)	9.05×10^{9}	[22]
$CO + OH = CO_2 + H$	(25)	1.79×10^{8}	[21]
$H + H + M = H_2 + M$	(26)	7.13×10^{8}	[21]

$$C_2H_5(s) + C_2H_5(s) = C_2H_6(s) + C_2H_4(s) \quad (32)$$

Clearly, reaction (32) is more important than reaction (31) because C_2H_5 would be more populated than CH_3.

Another possible mechanism of negative catalytic effect is the quenching of the O-containing radicals [13–15]. As discussed in Section 3.1, O-containing radicals (HO_2 and OH) are very important chain-carriers in the gas-phase reaction network. Since their reactions are so crucial in the activation/consumption of ethane and also in the subsequent reactions involving radicals and molecular products, the depletion in their concentration will lead to the decrease in the overall conversion of C_2H_6. In this study, however, we believe that the quenching of the O-containing radicals was less significant than that of the hydrocarbon radicals. As will be discussed later in the next section, under our experimental conditions, it is expected that surface-generated O-containing radicals will have more tendency to desorb from the catalyst surface. By considering the reversibility at the micro-molecular level, species easy to desorb must not adsorb easily. We therefore presume that the quenching of the oxygen-containing radicals had less effect on the inhibition of the gas-phase reactions observed in this study. Indeed, if HO_2/OH radicals are quenched more than the hydrocarbon radicals, the adverse effects of radical quenching must have been seen more profoundly on the formation rates of the degradation products

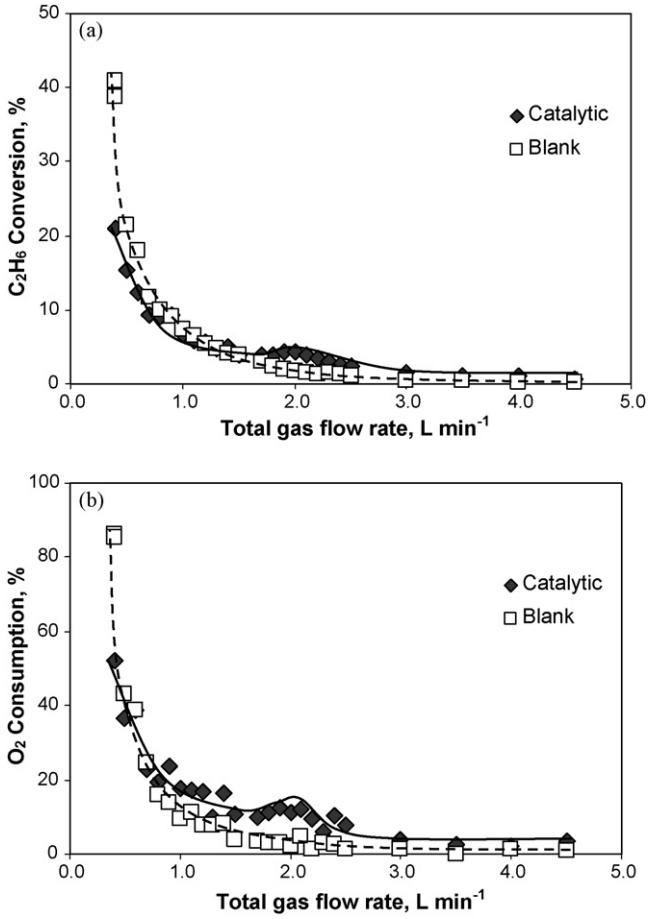

Fig. 3. Changes in ethane conversion (a) and oxygen consumption (b) with the total gas flow rate. T = 625 °C and $C_2H_6/O_2/Ar$ = 10/5/85.

(CO_x), due to their ability to facilitate deep oxidation [27], which is opposite to the experimental observation: the CO_2 formation rate actually increased due to the mesh catalyst (see Fig. 2).

3.2.2. Radical desorption—positive catalytic effects of mesh catalyst

Although the catalytic formation rate of C_2H_4 was lower than the blank at low gas flow rates (<1.7 L min^{-1}), an abrupt increase within a narrow flow rate range was observed when the flow rate was increased from 1.7 to 2.0 L min^{-1} (Fig. 2). This somewhat unusual "abrupt-effect" of gas flow rate is however completely unexplained by the theory of molecular species diffusion. This is because the mass transfer of molecular species to and from the catalyst alone would only exhibit a monotonic pattern in product formation rate [12], which is absolutely contrary to that observed in this study (Fig. 2).

A plausible explanation of the above observation is the change in the mass transfer of reactive radical species [8–12]. It is widely accepted [6,23] that the first step in the catalytic activation of saturated light hydrocarbon involves the breaking of C–H bond on an active surface site to form radicals. In the case of ethane, the molecule could dissociatively adsorb on the nickel metallic sites to form C_2H_5 and H radicals:

$$C_2H_6(g) = C_2H_5(s) + H(s) \quad (33)$$

The dissociative adsorption of C_2H_6 took place concurrently with the adsorption of another reactant O_2:

$$O_2(g) = 2O^-(s) \quad (34)$$

Therefore, an alternative step of C_2H_6 initiation is likely to be the reaction of C_2H_6 with the adsorbed oxygen atoms rather than its direct adsorption on the clean surface:

$$C_2H_6(g) + O^-(s) = C_2H_5(s) + OH(s) \quad (35)$$

In fact, it was found in the past [28–31] that oxygen species adsorbed on Ni surface has promoted C–H bond cleavage during the catalytic oxidation of methane.

Taking into account of reactions (33)–(35), it is clear that four types of reactive species, namely O(s), H(s), OH(s) and C_2H_5(s), were present on the catalyst surface. The tendency of each type of the species to desorb from the surface is largely determined by the strength of their bonding with Ni surface. The binding energies of O–Ni, H–Ni, OH–Ni and C_2H_5–Ni at zero coverage are 115, 63, 60.9 and 49 kcal/mol [32–34], respectively. The strength of OH–Ni bond is however very dependent on the surface oxygen coverage. Patrito et al. [35] have studied the energetics of hydroxyl adsorption on Ni and other metals. They found that high oxygen coverage lowers the OH–Ni bond strength from 60.9 kcal/mol at the zero coverage to 42.9 kcal/mol and 33.9 kcal/mol at the surface coverages of 0.6 and 1, respectively. The effects of oxygen coverage on the desorption of OH from Ni surface were observed by other researchers [36,37] where variation in the activation energy of OH desorption was reported.

Under our experimental conditions, low gas flow rates caused a thick and relatively stagnant gas film to be developed around the Ni

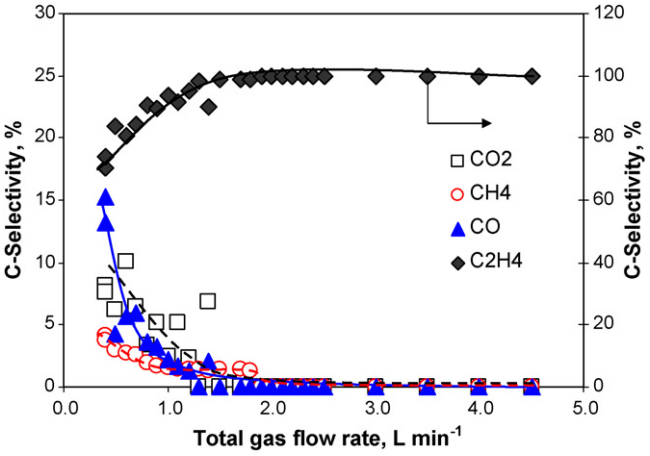

Fig. 4. Changes in C-selectivity with the total gas flow rate for the non-catalytic partial oxidation of ethane at 625 °C and $C_2H_6/O_2/Ar$ = 10/5/85.

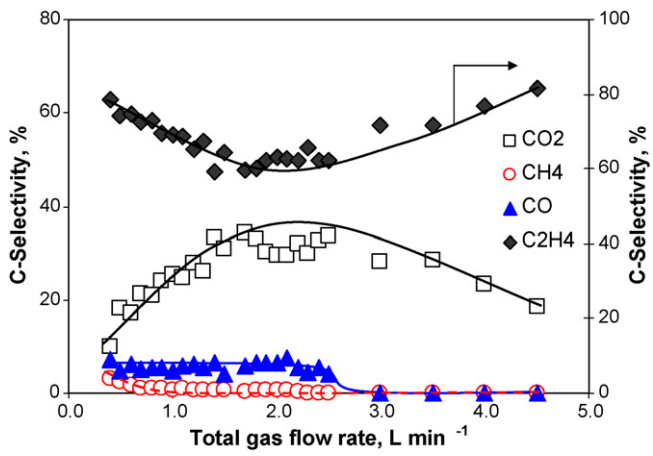

Fig. 5. Changes in C-selectivity with the total gas flow rate for the catalytic partial oxidation of ethane at 625 °C and $C_2H_6/O_2/Ar$ = 10/5/85.

wire mesh. The thick gas film would bring a difficulty for the radicals to diffuse into the bulk gas phase. Hence, few radicals would manage to desorb into the gas phase before they are consumed within the gas film. The increase in the gas flow rates (0.4 to ~2.0 L min^{-1}) decreased the thickness of the gas film around the mesh. The desorption and diffusion of the radicals into the gas phase then became easier [8–12]. Under our reaction conditions where high oxygen coverage is expected, we believe that OH radicals could desorb into the gas phase once the gas film thickness was reduced with increasing flow rate. The desorption of OH radicals from Ni surface has, in fact, been detected in the past studies [37,38] using a laser-induced fluorescence technique during the reaction of H_2 and O_2.

The desorption of OH radicals from the catalyst increased the concentration of OH radicals in the gas phase, which in turn resulted in the increases in the overall gas-phase reaction rate. As can be seen in reactions (9), (14), (15), (17)–(26), OH radicals are involved in both C_2H_6 consumption and many parts of deep oxidation mechanisms that lead to the formation of CO. Further reactions of OH with CO yield the thermodynamically stable CO_2 product together with H radical. One fate of H radicals would be their recombination to form H_2. Therefore, the desorption of OH radicals will increase the consumption of C_2H_6 (Fig. 3) and the formation of C_2H_4 and other products including CO, CO_2 and H_2 (Fig. 2). However, as OH radicals are involved in many rapid deep oxidation reactions [e.g. reactions (17)–(26)], the increased OH radical concentration in the gas phase would certainly speed up these deep oxidation reactions more than the reactions for the formation of C_2H_4 [e.g. reactions (9) and (4)]. This explains why the selectivity of C_2H_4 decreased while that of CO_2 increased (Fig. 5) as the flow rate was increased up to 2.0 L min^{-1}.

At very high gas flow rates (>2.0 L min^{-1}), the mass transfer resistance for the desorption of OH radicals from the catalyst surface is very small and no longer the rate-limiting step. The rates of OH radical generation on catalyst, which are chemical reactions, become the rate-limiting step. Hence, further increases in the total gas flow rate beyond 2.0 L min^{-1} would not result in further increases in the rate of OH radical generation and desorption. Instead, further increases in gas flow rate beyond this point would only dilute the concentrations of OH radical in the gas phase downstream the catalyst. The combined effects of decreased radical concentration

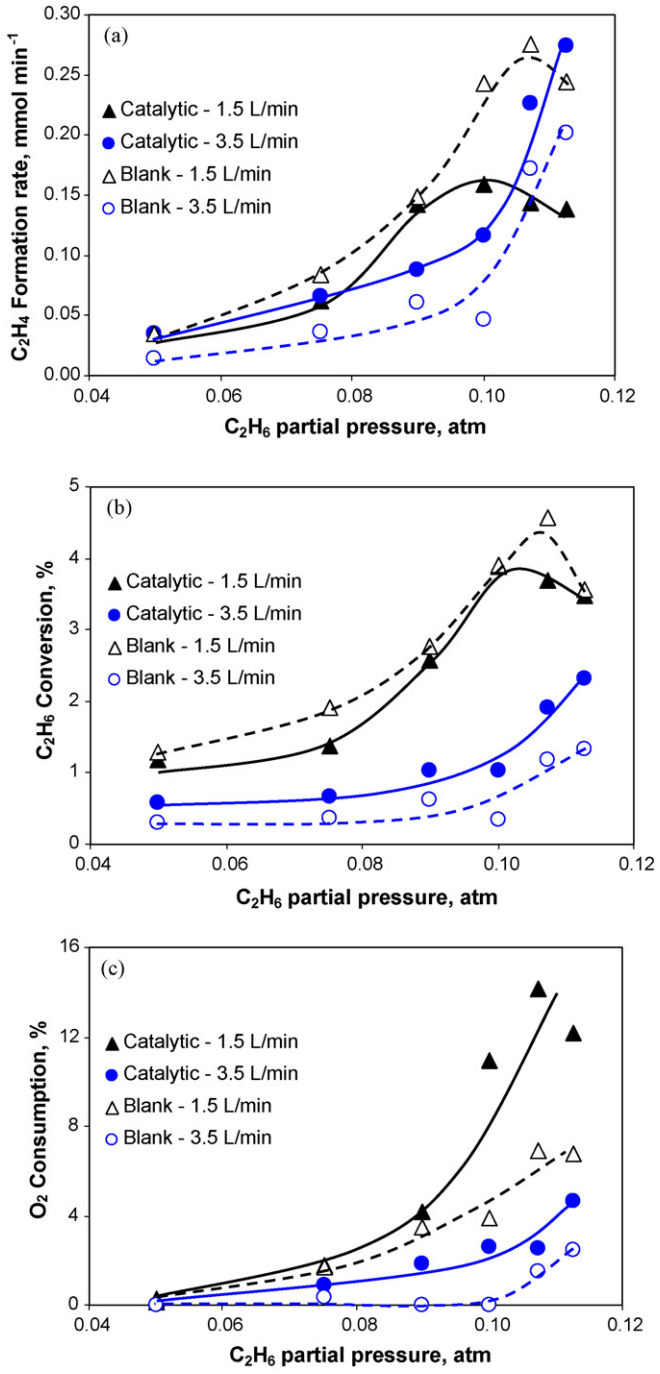

Fig. 6. Effects of C_2H_6 partial pressure on (a) C_2H_4 formation rate, (b) C_2H_6 conversion and (c) O_2 consumption at total gas flow rate of 1.5 L min^{-1} and 3.5 L min^{-1}.

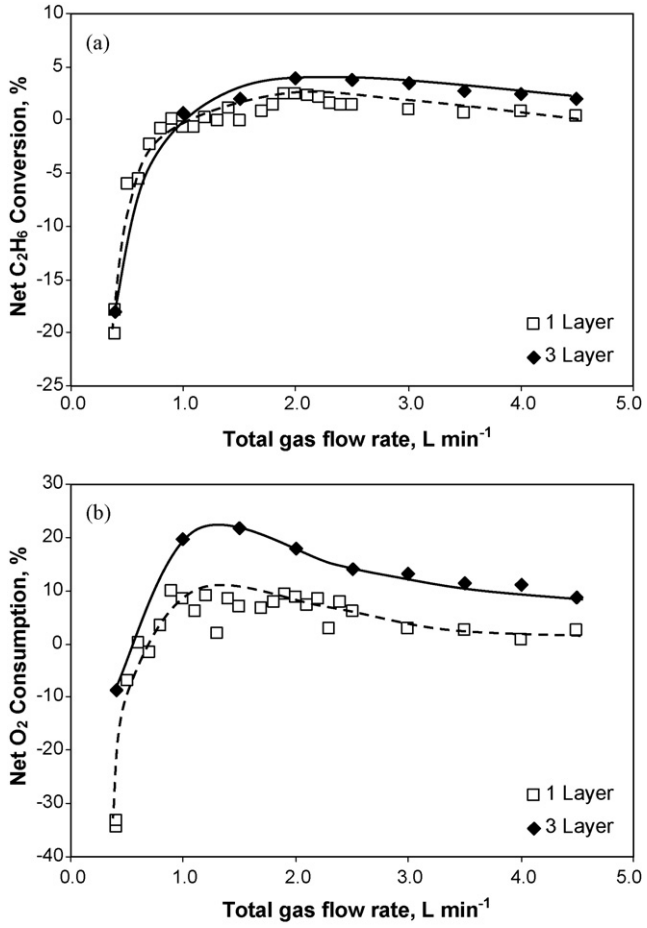

Fig. 7. Effects of increasing number of Ni mesh layers on (a) net-catalytic C_2H_6 conversion and (b) net-catalytic O_2 consumption.

and decreased residence time for subsequent reactions in the gas-phase reaction at the higher flow rates (beyond 2.0 L min^{-1}) result in decreases in the reaction rates. The explanation outlined here provides a plausible explanation for the decreases in the catalytic formation rates of all products (C_2H_4, CH_4, CO, CO_2 and H_2) at flow rates higher than 2.0 L min^{-1} (Fig. 2). The changes in product selectivity (Fig. 5) with increasing gas flow rate (>2.0 L min^{-1}) are due to two related reasons. Firstly, decreased OH radical concentration due to the dilution effect mentioned above would also decrease the relative importance of deep oxidation reactions [reactions (17)–(26)]. This contributes to the increases in the selectivity of C_2H_4 and the decreases in the selectivities of CO_2 and CO (Fig. 5) from the catalytic reactions at total gas flow rates higher than 2.0 L min^{-1}. Secondly, further increase in the gas flow rate beyond 2.0 L min^{-1} would mean shorter time spent in the heated zone of the reactor by C_2H_4 product molecules, allowing them to exit from the reactor before they were destroyed to CO_x, H_2 and H_2O.

3.2.3. *Effects of reactant partial pressures*

We have carried out experiments at different ethane/oxygen partial pressures in order to justify the above discussion made on the radical quenching and radical desorption. With the total pressure remained at atmospheric, the reactant partial pressures were varied by changing the relative proportions of C_2H_6 and O_2 while the percentage of argon dilution was kept at 85%. In this examination, two different flow rates were chosen (1.5 and 3.5 L min^{-1}) to represent two different regions: the region of negative catalytic effect and the region of positive catalytic effect respectively.

As noted in the previous sections, gas-phase activation via reactions (1) and (3) are dominant at lower flow rates. Increasing C_2H_6 partial pressure will promote these activation reactions. However, due to the importance of O_2 in the propagation steps, continued increases in the C_2H_6 partial pressure would not always result in continuous increases in the overall reactions rate. As is clearly shown in Fig. 6, the formation rates of C_2H_4 from the catalytic and non-catalytic reactions increased initially as the C_2H_6 partial pressure was increased. Further increases in the C_2H_6 partial pressure for the reactions at 1.5 L min^{-1} however resulted in the catalytic formation rate of C_2H_4 to approach its maximum value. It is also obvious in Fig. 6 that the formation rate of C_2H_4 and the conversion of C_2H_6 were always lower in the presence than in the absence of a mesh catalyst during reactions at 1.5 L min^{-1} even around the maximum values. This has given further evidence on the dominance of the gas phase reactions at lower flow rate region and the effect of radical quenching during catalytic reactions in this region.

The reactions in the higher flow rate region are more influenced by the activation on the catalyst surface and the desorption of radicals. At 3.5 L min^{-1}, the catalytic reaction rates at all C_2H_6 partial pressures studied showed larger values than those obtained from the blank experiments. Within this range of C_2H_6/O_2 ratio (partial pressures), O_2 did not become a limiting reactant on the catalyst surface, as is evidenced by its low conversion (Fig. 6). Increasing C_2H_6 partial pressure could promote surface activation via reaction (35) and consequently resulted in the increased formation of surface-generated OH radicals which subsequently desorbed into the gas phase to enhance ethane consumption via reaction (9). It is clear that two consequences existed when the C_2H_6 partial pressure was increased at 3.5 L min^{-1}. One was the increase in ethane activation on the catalyst surface and another was the increase in the reaction of ethane with OH radicals in the gas phase. These two effects combine to provide a conceivable explanation to the non-linear increase (Fig. 6) of catalytic reaction rates with increasing C_2H_6 partial pressure observed at the flow rate of 3.5 L min^{-1}.

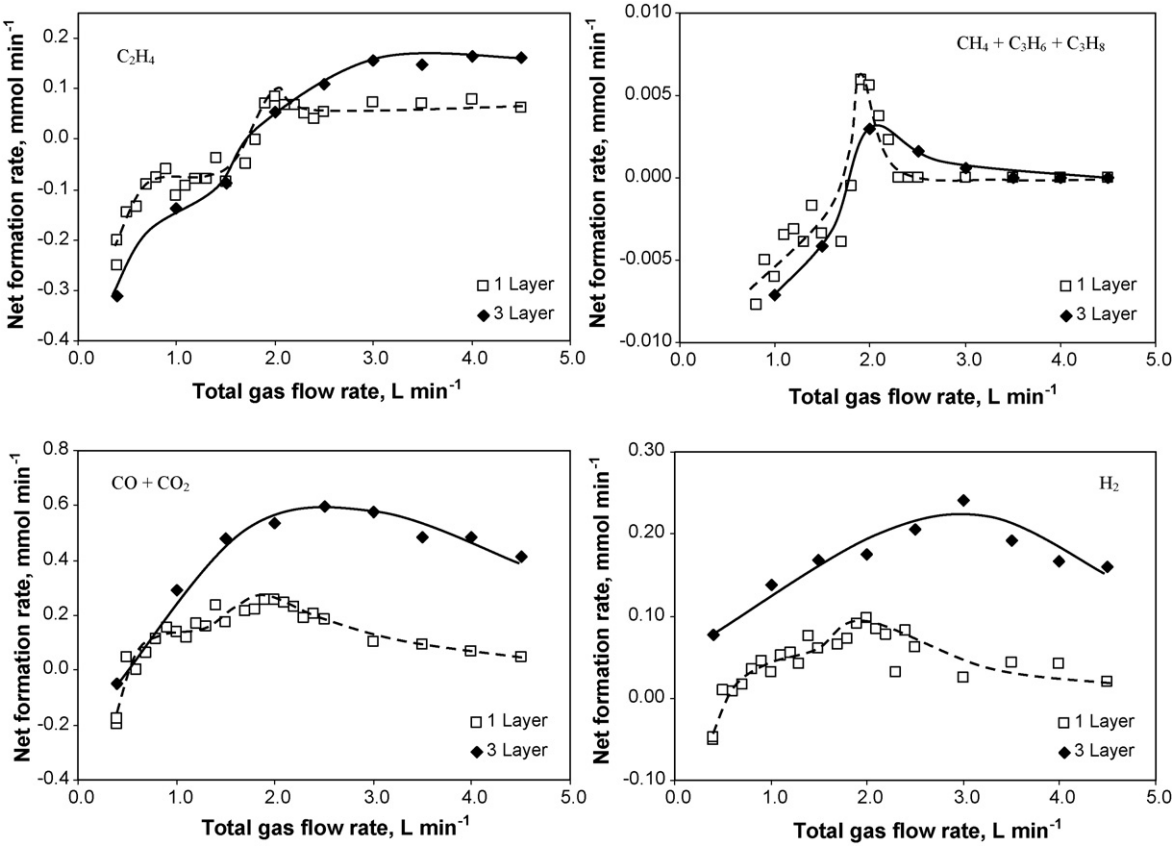

Fig. 8. Comparison of product net-catalytic formation rates from reactions with 1 layer of mesh catalyst and 3 layers of mesh catalyst.

3.3. Further study using 3 layers of nickel mesh

Further investigation was carried out by employing three pieces of nickel mesh. In these experiments, the meshes were placed in the isothermal zone with a distance of about 5 mm apart. The first layer of mesh was always ensured to be in the position identical to that in the experiments using one piece of mesh. The second and third pieces were down stream (physically on top of) of the first (see Fig. 1). The "net" catalytic contributions in term of reactant conversions and product formation rates were calculated by subtracting the rates of the blank experiments from the ones obtained with Ni mesh (1 or 3 layers) at the same flow rate (Figs. 7 and 8). To our surprise, increasing catalyst surface area by increasing the number of mesh pieces did not always bring a proportional increase in reactant conversion. As is shown in Fig. 7, extra catalyst surface area had a promoting effect on ethane and oxygen conversion at higher flow rate (>1.5 L min^{-1}) region. However, at the lower flow rate (<0.8 L min^{-1}) region, reactant conversions (especially C_2H_6) were much lower than those of the blank experiments.

As can be seen in Fig. 8, the use of three layers of nickel mesh tended to give higher formation rates of CO_2 and H_2 than that obtained with a single layer of mesh. The formation rates of other products (mainly C_2H_4) however only increased at high flow rates (>2.0 L min^{-1}) but dropped significantly at low flow rates (<2.0 L min^{-1}). The C_2H_4 formation rates at high flow rates though did not increase to the same magnitude as the increases in CO_x and H_2. The results using 3 layers of mesh support our discussion presented in previous sections on the roles of mesh catalyst. In particular, the large negative impact on the formation rates of hydrocarbon products at lower flow rates further confirms that the radical species which has been quenched most by the catalyst surface at lower flow rates region must be hydrocarbon radicals (e.g. C_2H_5). It is also clear that the desorption of surface-generated O-containing radicals (OH radicals) has resulted in the enhanced reaction rates to form CO_x and H_2 more than C_2H_4. Some C_2H_5 radicals desorbed form the earlier catalyst layer may have been quenched by the next catalyst layer. This explains why C_2H_4 formation rates at high gas flow rates did not increase to the same magnitude as the increase in CO_x and H_2 when the number of catalyst layer was increased from one layer to three layers.

The void regions in between mesh pieces at least partly represent the situations inside the pores of a porous catalyst through which radicals have to diffuse to reach the bulk stream of the gas flow. Inside these regions, radicals could have migrated from one catalyst surface to another catalyst surface and many reactions could take place on them before they exit the catalyst zone. Although the actual situations inside the pore structure of a porous catalyst are much more complicated than the (5 mm apart) space between the mesh pieces, the heterogeneous-generation, desorption and quenching of the radicals observed from the experiments using three layers of mesh have nevertheless given some insights into the potential reaction mechanisms in the pores of a traditional porous catalyst.

4. Conclusions

A catalyst may influence the gas-phase radical chain reactions in two different ways. In this study using a non-porous nickel mesh catalyst for the partial oxidation of ethane, the exact catalytic effects of the catalyst strongly depended on the flow rate of gas reactants passing through the mesh. At a low gas flow rate, the nickel mesh catalyst showed negative effects for the oxidation of ethane due to the quenching of hydrocarbon radicals (e.g. C_2H_5) by the catalyst. At a high gas flow rate, the same catalyst showed positive catalytic effects due to the selective/preferential desorption of some radicals such as OH radicals from the catalyst surface. The overall effects of radical desorption would be the preferential increases in the formation of terminal products (CO_2 and H_2) relative to the formation of C_2H_4. Our results will be valuable both in the fundamental research for the rethinking of the reaction mechanism and in the applied research for the improvement in catalyst and process design related to any catalytic conversion of light hydrocarbons.

Acknowledgements

This study was financially supported by a grant from the Australian Research Council (DP0556095). S.S.A. Syed-Hassan is grateful to the scholarship award by the Malaysian Ministry of Higher Education and the University Technology MARA.

References

[1] T. Ren, M. Patel, K. Blok, Energy 31 (2006) 425–451.
[2] M. Eramo, Oil Gas J. 103 (2005) 52–60.
[3] E. Morales, J.H. Lunsford, J. Catal. 118 (1989) 255–265.
[4] J.H. Lunsford, Langmuir 5 (1989) 12–16.
[5] K.D. Campbell, J.H. Lunsford, J. Phys. Chem. 92 (1988) 5792–5796.
[6] K.T. Nguyen, H.H. Kung, J. Catal. 122 (1990) 415–428.
[7] F. Gudmundson, J.L. Persson, M. Försth, F. Behrendt, B. Kasemo, A. Rosén, J. Catal. 179 (1998) 420–430.
[8] E.B.H. Quah, C.Z. Li, Appl. Catal. A: Gen. 250 (2003) 83–94.
[9] E.B.H. Quah, C.Z. Li, Appl. Catal. A: Gen. 258 (2004) 63–71.
[10] E.B.H. Quah, C.Z. Li, Int. J. Chem. Kinet. 35 (2003) 637–646.
[11] E.B.H. Quah, J.F. Mathews, C.Z. Li, J. Catal. 197 (2001) 315–323.
[12] W.J. Lee, C.Z. Li, Appl. Catal. A: Gen. 316 (2007) 90–99.
[13] P.M. Couwenberg, Q. Chen, G.B. Marin, Ind. Eng. Chem. Res. 35 (1996) 415–421.
[14] P.M.P. Couwenberg, Q. Chen, G.B. Marin, Ind. Eng. Chem. Res. 35 (1996) 3999–4011.
[15] Y.S. Su, J.Y. Ying, W.H. Green, J. Catal. 218 (2003) 321–333.
[16] R.C. Burch, M.E. Crabb, Appl. Catal. A: Gen. 97 (1993) 49–65.
[17] W.J. Lee, C.-Z. Li, Carbon 46 (2008) 1208–1217.
[18] D.M. Kulich, J.E. Taylor, Int. J. Chem. Kinet. 7 (1975) 895–905.
[19] J.E. Taylor, D.M. Kulich, Int. J. Chem. Kinet. 5 (1973) 455–468.
[20] P. Dagaut, M. Cathonnet, J.C. Boettner, Int. J. Chem. Kinet. 23 (1991) 437–455.
[21] Y. Hidaka, K. Sato, H. Hoshikawa, T. Nishimori, R. Takahashi, H. Tanaka, K. Inami, N. Ito, Combust. Flame 120 (2000) 245–264.
[22] C.K. Westbrook, F.L. Dryer, Prog. Energy Combust. Sci. 10 (1984) 1–57.
[23] R. Burch, M.J. Hayes, J. Mol. Catal. A: Chem. 100 (1995) 13–33.
[24] L. Leveles, K. Seshan, J.A. Lercher, L. Lefferts, J. Catal. 218 (2003) 296–306.
[25] E. Heracleous, A.A. Lemonidou, Appl. Catal. A: Gen. 269 (2004) 123–135.
[26] E. Heracleous, A.A. Lemonidou, Catal. Today 112 (2006) 23–27.
[27] J.C. Mackie, J.G. Smith, P.F. Nelson, R.J. Tyler, Energy Fuels 4 (1990) 277–285.
[28] G. Krishnan, H. Wise, Appl. Surf. Sci. 37 (1989) 244–249.
[29] C.T. Au, M.S. Liao, C.F. Ng, J. Phys. Chem. A 102 (1998) 3959–3969.
[30] Y.H. Hu, E. Ruckenstein, Catal. Lett. 34 (1995) 41–50.
[31] O. Dewaele, G.F. Froment, J. Catal. 184 (1999) 499–513.
[32] E. Shustorovich, Adv. Catal. 37 (1990) 101–163.
[33] A.A. Zeigarnik, C. Callaghan, R. Datta, I. Fishtik, E. Shustorovich, Kinet. Catal. 46 (2005) 509–515.
[34] A.T. Bell, E. Shustorovich, Surf. Sci. 235 (1990) 343–350.
[35] E.M. Patrito, P.P. Olivera, H. Sellers, Surf. Sci. 306 (1994) 447–458.
[36] H. Yang, J.L. Whitten, J. Phys. Chem. B 101 (1997) 4090–4096.
[37] J.T. Keiser, M.A. Hoffbauer, M.C. Lin, J. Phys. Chem. 89 (1985) 2635–2638.
[38] S. Ljungstrom, J. Hall, B. Kasemo, A. Rosen, T. Wahnstrom, J. Catal. 107 (1987) 548–556.
[39] Y. Hidaka, K. Kimura, K. Hattori, T. Okuno, Combust. Flame 106 (1996) 155–167.
[40] S. Mousavipour, J. Phys. Chem. A 107 (2003) 8566–8574.